Electronic Supplementary Material (ESI) for Dalton Transactions.

Supporting information

A study on the influence of ligand variation on formamidinate complexes of yttrium: New precursors for atomic layer deposition of yttrium oxide

Sebastian M. J. Beer[a], Nils Boysen,[a] Arbresha Muriqi[b], David Zanders[a], Thomas Berning[c], Detlef Rogalla[d], Claudia Bock[c], Michael Nolan[b], Anjana Devi[a*]

[a] Inorganic Materials Chemistry, Ruhr University Bochum, Universitätsstr. 150, 44801 Bochum, Germany

Tyndall National Institute, University College Cork, Lee Maltings, Cork T12 R5CP, Ireland

[c] Lehrstuhl für Mikrosystemtechnik, Ruhr University Bochum, Universitätsstr. 150, 44801 Bochum, Germany

[d] RUBION, Ruhr University Bochum, Universitätsstr. 150, 44801 Bochum, Germany

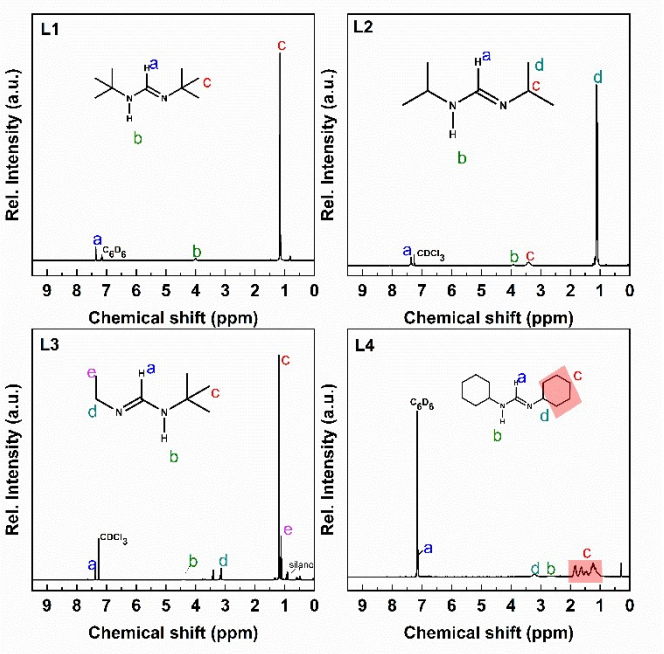

Figure SI 1: ^{1}H-NMR (400 MHz) of the formamidine ligands **L1-L4**, recorded in C_6D_6 (**L1, L4**) and $CDCl_3$ (**L2, L3**).

FTIR: Fourier-transform infrared-spectroscopy was also carried out for the formamidine ligands **L1** – **L4** and Y formamidinate complexes **1**–**4** suiting the literature (Taylor, M. J. *et al*., J. Che. Soc., *Faraday Trans*., **1997**, 93, 2503-2507). as shown in Figure SI 2. In summary, the broad N-H vibration mode around 3250 cm^{-1} was only detected in the spectra of the free ligands **L1**–**L4**, indicating a successful complexation of the Y metal with the formamidinate ligands for complexes **1**–**4**. This is supported by the fact, that for compound **1**–**4**, the C=N (1660 cm^{-1}) double bond vibration band intensity decreases, while the N-C-N vibration around 1535 cm^{-1} becomes more pronounced. Hence, a stronger π-electron delocalization in the NCN backbone can be expected which is in accordance with the structural prediction shown in the DFT calculations discussed below.

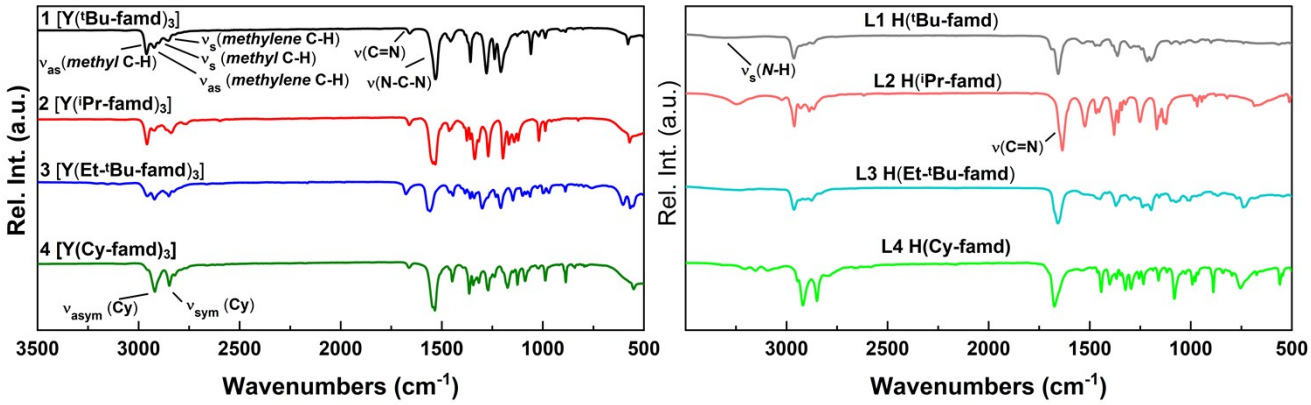

Figure SI 2: FT-IR of the metalorganic yttrium complexes **1**-**4** (left) and the protonated ligands **L1-L4** (right).

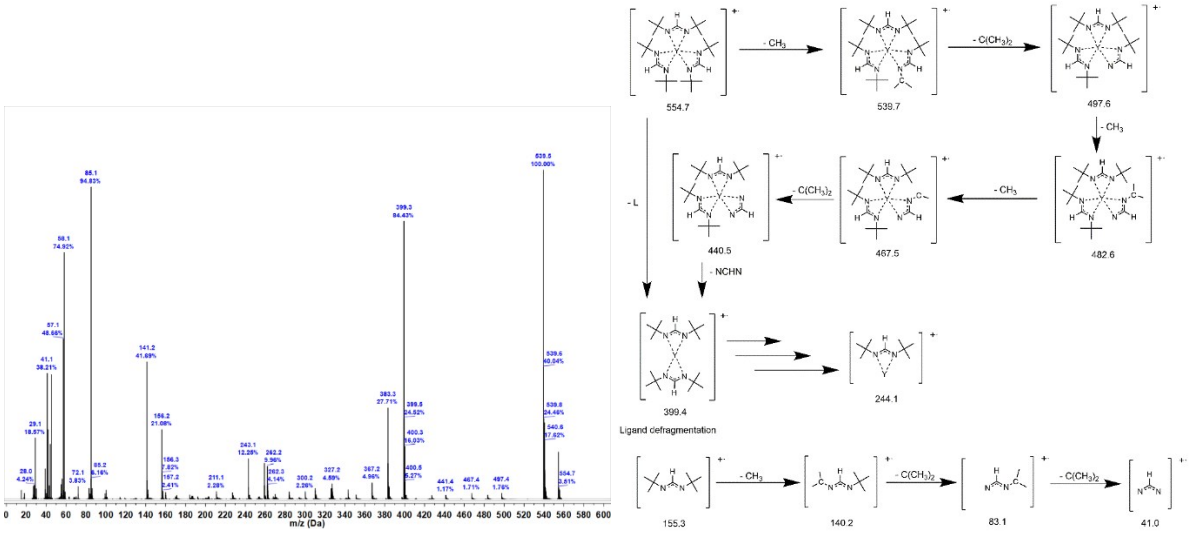

Figure SI 3: EI-MS spectrum (70 eV) (left) and proposed fragmentation pattern (right) of compound [Y(tBu-famd)$_3$] **1**.

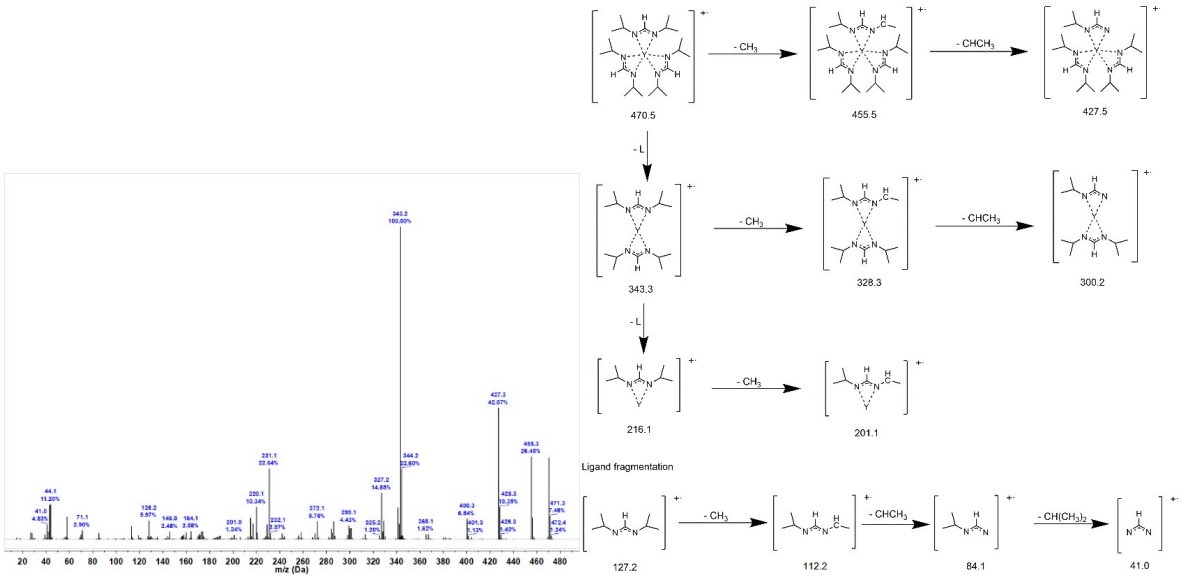

Figure SI 4: EI-MS spectrum (70 eV) (left) and proposed fragmentation pattern (right) of compound [Y(^{i}Pr-famd)$_3$] **2**.

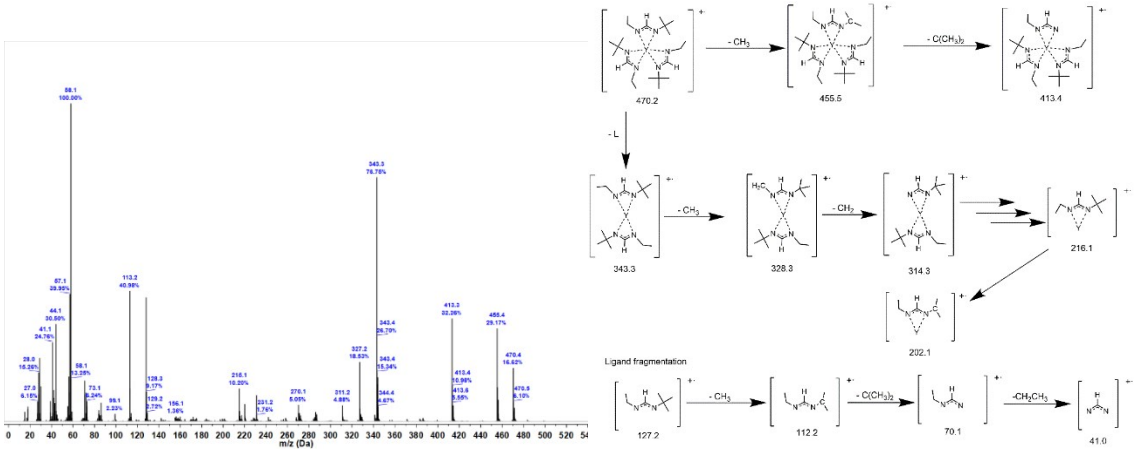

Figure SI 5: EI-MS spectrum (70 eV) (left) and proposed fragmentation pattern (right) of compound [Y(Et-^{t}Bu-famd)$_3$] **3**.

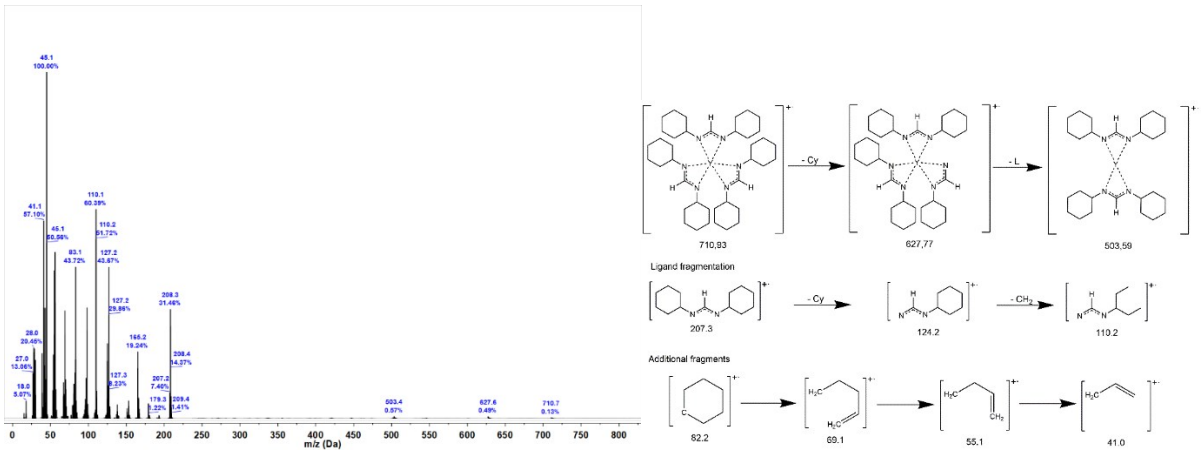

Figure SI 6: EI-MS spectrum (70 eV) (left) and proposed fragmentation pattern (right) of compound [Y(Cy-famd)$_3$] **4**.

Table SI 1: Summary of EI-MS fragments of compound **1 – 4**.

	[Y(^{t}Bu-famd)$_3$] **1**		[Y(^{i}Pr-famd)$_3$] **2**		[Y(Et-^{t}Bu-famd)$_3$] **3**		[Y(Cy famd)$_3$] **4**	
Fragment	m/z	Rel Int (%)	m/z	Rel Int (%)	m/z	Rel Int (%)	m/z	Rel Int (%)
[YL_3]	554.5	14.24	470.3	26.13	470.4	16.6	710.7	0.13
[YL_3 - CH_3]	539.6	100	455.3	28.45	455.4	29.17		
[YL_3 - R^1]			427.3	42.07	413.3	32.26	627.6	0.49
[YL_2]	399.3	84.43	343.2	100	343.3	76.75	503.4	0.57
[YL^2 - CH_3]	383.3	27.71	327.2	14.85	327.2	18.53		
[YL]	243.1	12.25	215.1	6.88	215.1	10.2		
[L]	156.2	21.08	128.2	5.97	128.2	38.19	208.3	31.46
[L - CH_3]	141.2	41.69	113.1	4.22	113.2	40.98		

Table SI 2: Y-N bond lengths of **1**-**4** under vacuum conditions.

	[Y(^{t}Bu-famd)$_3$] **1**	[Y(^{i}Pr-famd)$_3$] **2**	[Y(Et-^{t}Bu-famd)$_3$] **3**	[Y(Cy famd)$_3$] **4**
Y-N1	2.40 Å	2.37 Å	2.38 Å	2.39 Å
Y-N2	2.39 Å	2.38 Å	2.38 Å	2.39 Å
Y-N3	2.40 Å	2.38 Å	2.38 Å	2.36 Å
Y-N4	2.39 Å	2.39 Å	2.39 Å	2.41 Å
Y-N5	2.39 Å	2.39 Å	2.38 Å	2.38 Å
Y-N6	2.39 Å	2.39 Å	2.39 Å	2.39 Å

Table SI 3: N-Y-N bite angle of **1**-**4** under vacuum conditions.

	[Y(^{t}Bu-famd)$_3$] **1**	[Y(^{i}Pr-famd)$_3$] **2**	[Y(Et-^{t}Bu-famd)$_3$] **3**	[Y(Cy famd)$_3$] **4**
N1-Y-N2	56.9 °	57.1 °	57.0 °	57.0 °
N3-Y-N4	56.9 °	57.0 °	57.0 °	56.8 °
N5-Y-N6	56.9 °	58.0 °	57.0 °	56.9 °

Table SI 4 Computed bond dissociation energies of **1**-**4** for the cleavage of the first ligand under vacuum conditions.

	E_{ligand} (kJ/mol)
[Y(^{t}Bu$_2$-famd)$_3$] **1**	493.59
[Y(^{i}Pr$_2$-famd)$_3$] **2**	488.34
[Y(Et-^{t}Bu-famd)$_3$] **3**	493.59
[Y(Cy_2-famd)$_3$] **4**	472.58

Table SI 5: Y-N and Y-OH distances of precursor **1-4** after the reaction with H_2O under vacuum conditions.

	[Y(^{t}Bu-famd)$_3$] **1**	[Y(^{i}Pr-famd)$_3$] **2**	[Y(Et-^{t}Bu-famd)$_3$] **3**	[Y(Cy famd)$_3$] **4**
Y-N1	2.45 Å	2.45 Å	2.38 Å	2.38 Å
Y-N2	2.40 Å	2.36 Å	2.41 Å	2.43 Å
Y-N3	2.39 Å	2.39 Å	2.43 Å	2.41 Å
Y-N4	2.44 Å	2.43 Å	2.39 Å	2.41 Å
Y-N5	2.53 Å	2.53 Å	2.47 Å	2.46 Å
Y-OH	2.15 Å	2.15 Å	2.15 Å	2.15 Å

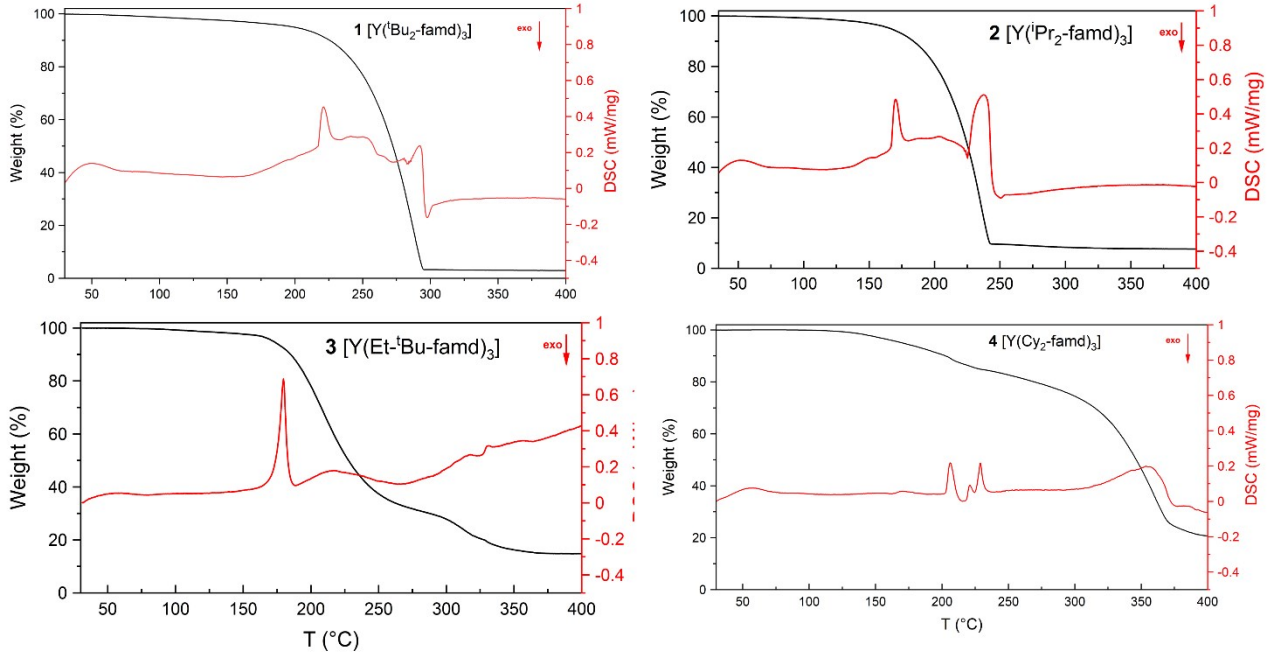

Figure SI 7: TG (black) and DSC (red) (TG/DSC) of compound **1**-**4**.

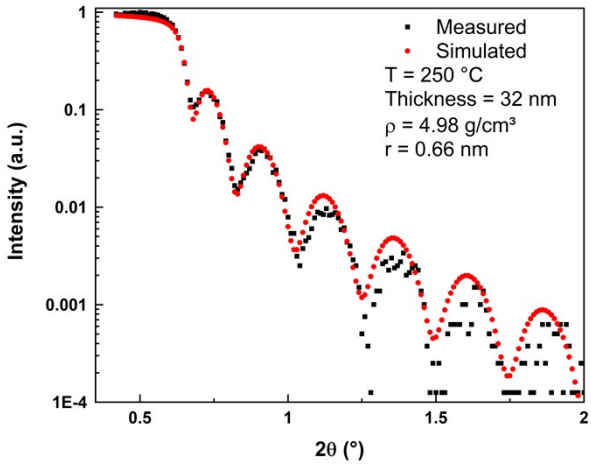

Figure SI 8: Measured (black dots) and simulated XRR curves and obtained film parameters (temperature T, thickness, density ρ and roughness r) from a deposition using **1** at 250 ° substrate temperature.

Table SI 6: Composition of Y_2O_3 films grown on Si(100) at 175 °C, 250 °C and 300 °C derived from RBS/NRA and XPS analysis. XPS composition is shown for as deposited (a.d.) and sputtered (sp.) films.

Method	T_{dep} (°C)		Composition (at.%)				O/Y ratio
			Y	O	C	N	
RBS/NRA	**175**		34.2	61.4	2.9	1.5	1.79
	250		37.6	60.1	1.5	0.9	1.60
	300		37.0	59.8	1.7	1.5	1.62
XPS	***250***	*a.d.*	*35.9*	*56.3*	*7.8*	*n.d.*	*1.58*
		sp.	*43.1*	*55.5*	*1.4*	*n.d.*	*1.29*
	300	*a.d.*	*31.4*	*47.2*	*21.4*	*n.d.*	*1.50*
		sp.	*44.8*	*51.6*	*3.6*	*n.d.*	*1.15*

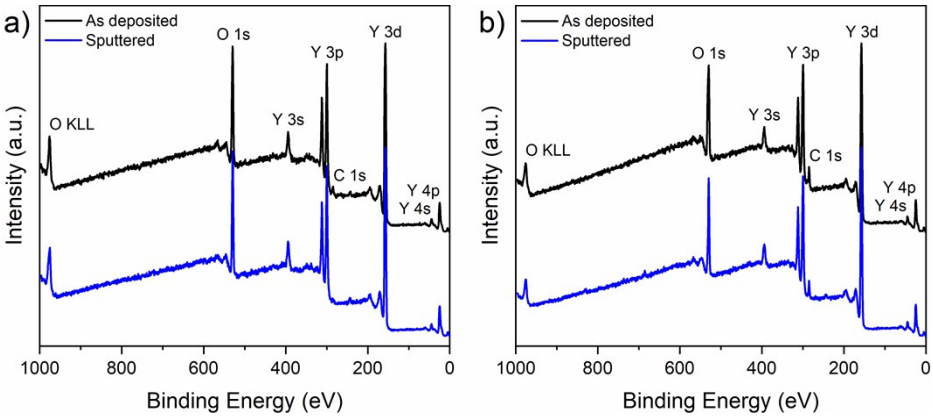

Figure SI 9: Survey spectra of Y_2O_3 thin films deposited on Si(100) at a) 250 °C and b) 300 °C. The survey scans are shown for the untreated and sputtered surfaces. Labels are assigned to the respective core levels and Auger lines.

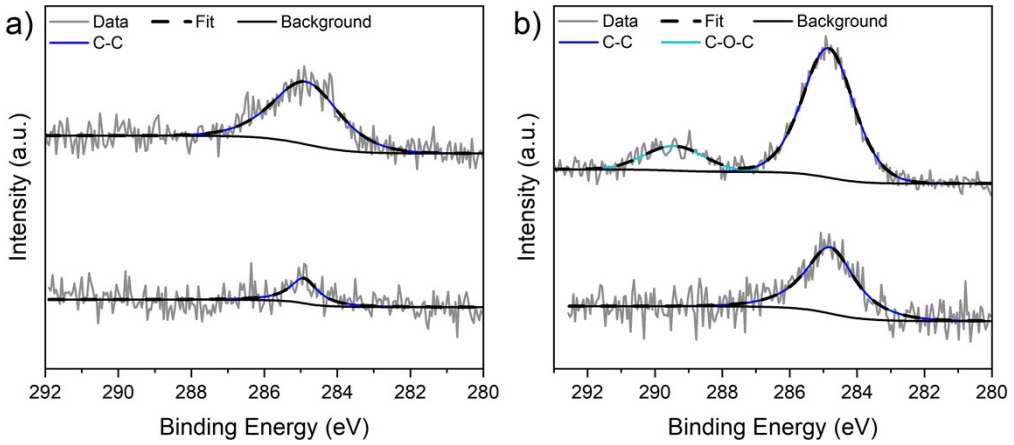

Figure SI 10: C 1s core level spectra recorded for Y_2O_3 thin films deposited on Si(100) at a) 250 °C and b) 300 °C. The C 1s core level recordings are displayed for the untreated and sputtered surfaces and indicate only minor carbon incorporation into the thin films.

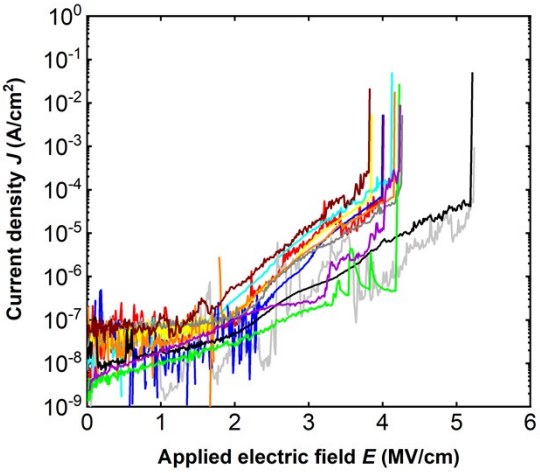

Figure SI 11: Leakage current density J as a function of the electric field E for several MIS devices incorporating Y_2O_3 (d =20 nm) deposited at T = 300 °C. Each color represents a J-E characteristic of an individual device.